

# **Impairment of Erythrocyte Deformability Observed in Type 2 Diabetic Patients with Clustering Diabetic Complications**

## **ABSTRACT**

**Aims:** Hemorheologic and microvascular dysfunction are interdependent in type 2 diabetic patients. However, exact mechanisms explaining this interaction remains unclear. This study aimed to investigate the impairment of erythrocyte deformability under concurrent recording of electrocardiogram (ECG), since heart-rate-corrected QT interval (QTc interval) prolongation reflects autonomic and microvascular dysfunction in diabetic patients.

**Methodology:** The erythrocyte deformability was investigated on the day of digital ECG recording in diabetic (n = 215) and control (n = 88) groups of outpatients using specific filtration technique. Significant contributors to the erythrocyte deformability were analyzed by multivariate analysis. **Results:** Difference of mean erythrocyte deformability in the diabetic vs. control group did not reach the statistical significance, but the difference was significant in comparison of diabetic smokers vs. non-smokers and of diabetic patients with vs. without diabetic complications. Impaired diabetic erythrocyte deformability was dependent mostly on the glycated hemoglobin (HbA1c), and negative correlation between QTc interval and the deformability was marginal. **Conclusions:** Erythrocyte deformability was not necessarily impaired in diabetic patients under the intensive antidiabetic medication. However, this deformability was impaired in diabetic smokers and diabetic patients with clustering of complications. Future studies are required for hemorheologic and microvascular interaction leading to the impaired diabetic microcirculation.

*Keywords: Deformability; diabetes; erythrocytes; microcirculation.*

---

## **1. INTRODUCTION**

Type 2 diabetes mellitus is a world-wide growing healthcare burden, and lifestyle intervention is emergent for diabetes prevention [1]. Diabetic complications such as retinopathy, nephropathy and neuropathy are based on microangiopathy and dependent on glycemic control over time, which is known as a metabolic memory. Diabetes is associated with various hemorheologic disorders, i.e., these include platelet activation and increased whole blood viscosity and plasma viscosity. With respect to erythrocytes, morphology is changed, and deformability tends to decrease [2,3]. The deformability of erythrocytes

passing through microvasculature is a prerequisite of microcirculation, and this deformability in diabetic patients has been so far investigated. However, the results are confusing because of diverse hemorheologic methodologies, such as filtration study, microchannel study and ektacytometry [2,4,5]. The concept of erythrocyte deformability is not strictly defined as a physical quantity, and the evaluation of deformability depends on the hemorheologic techniques showing individual sensitivity and reproducibility. Since circulating erythrocytes show bending deformation presenting parachute-like configuration in microvasculature, erythrocyte deformability *in vivo* can be quantified by filterability during passage of intact erythrocytes through a highly sensitive and quantitative nickel mesh filter [6,7]. Diabetic complications are based on microangiopathy, and diabetic erythrocytes with poor deformability underlie stagnant microcirculation and chronic tissue hypoxia. However, hemorheologic impact of less deformable erythrocytes on diabetic complication is not fully elucidated. We hypothesized that less deformable erythrocytes avoid passing through critically narrow microvasculature, which causes microvascular dysfunction under the insufficient capillary blood flow in diabetic patients. Therefore, this study aimed to test this hypothesis in comparison of erythrocyte deformability and surrogate of microvascular function in diabetic with non-diabetic patients.

## 2. METHODOLOGY

### 2.1 Selection of Subjects

The present study was performed according to the Declaration of Helsinki (2000) from April 2015 to September 2017. The study population consisted of 174 Japanese patients with type 2 diabetes mellitus and 51 non-diabetic, age-matched control subjects. These patients were under the regular visit to the outpatient division of BOOCS Clinic in Fukuoka City. Type 2 diabetes was defined as fasting serum glucose > 126 mg/dl, casual serum glucose > 200 mg/dl, percentage of hemoglobin A1c relative to the total hemoglobin which was estimated according to National Glycohemoglobin Standardization Program that is termed HgA1c(NGSP) > 6.5% and/or current antidiabetic medication. Diabetic patients were treated under the discretion of the treating physicians in this clinic. Diabetic complications of retinopathy and nephropathy were evaluated by experienced diabetologists by means of ophthalmoscopy and urine albumin excretion, respectively. Diabetic neuropathy was estimated by recording digital electrocardiogram (ECG) to obtain the coefficient of variance of R-R intervals (CVRR: %) under sinus rhythm, because CVRR is an age-dependent representative measure of heart rate variability, i.e., neuropathy was defined as the ratio of actual CVRR and the CVRR predicted by age < 0.8 as in literature [8].

All patients' data were collected by routine laboratory tests performed under the monthly visit to the clinic. In addition to the type 2 diabetes, other conventional coronary risk factors were evaluated, i.e., age, gender, smoking status, height and body weight (BW) were registered. Body mass index (BMI) was calculated by BW (kg) divided by square of height (m). These demographic variables of the enrolled participants were extracted from personal medical records. Blood pressure (BP: mmHg) was measured by sphygmomanometer in sitting position after taking a few minute rest. Blood and biochemical laboratory, urinalysis, chest X-ray and transthoracic echocardiographic examination were performed routinely in all the enrolled patients.

Hypertension was defined as casual blood pressure > 140 / 90 mmHg and/or treatment with antihypertensive drugs. Dyslipidemia was also defined as serum LDL cholesterol > 140 mg/dl, serum HDL cholesterol < 40 mg/dl and/or prescription of lipid-lowering drugs [9]. Exclusion criteria for diabetic patients included uncontrolled diabetic status (i.e., ketoacidosis, diabetic coma and frequent hypoglycemic episodes) and advanced diabetic

nephropathy requiring hemodialysis. Patients under the treatment with drugs affecting on QT interval such as probucol, antiarrhythmic drugs, antipsychotic drugs, antifungal and antibiotic agents were also excluded. Antidiabetic medications and lifestyle including smoking were not altered in any patients during the study period. Signed informed consent was obtained from each subject prior to the enrollment into the study. The study design was approved by the internal ethics committee of The Institute of Rheological Function of Foods Co. Ltd (Hisayama, Fukuoka, Japan).

## 2.2 ECG Recordings

Enrolled subjects underwent resting 12-lead ECG on the day of venous blood sampling for erythrocyte deformability estimation. ECG was recorded in supine position using digital ECG recorder (CARDISUNY C310, FUKUDA ME, Tokyo, Japan), and was printed at a paper speed of 25 mm/sec and amplitude of 10 mm/mV or 5 mm/mV as appropriate. Absolute QT interval (msec) is electrically defined cardiac ventricular contraction time and measured from the beginning of the QRS complex to the end of the T wave on ECG. QT interval is dependent highly on the preceding R-R interval (msec) and hence was corrected automatically by the Bazett's formula (QTc: msec), where  $QTc = QT/RR^{1/2}$ . CVRR reflecting heart rate variability was also obtained automatically after a few minutes monitoring of ECG by accumulating 100 cardiac beats under sinus rhythm. ECG data were transferred using A/D converter, stored automatically to a personal computer (VAIO, model SVP132A16N, SONY<sup>®</sup>, Tokyo, Japan), and diagnosed based on Minnesota code. Thereafter, ECG recordings were reviewed by experienced cardiologists in a blind manner. ECG exclusion criteria were documented atrial fibrillation and other sustained arrhythmias, manifest WPW syndrome, right or left bundle branch block, atrioventricular block with its degree of second or more and intraventricular conduction disturbance showing QRS width > 120 msec. QT and QTc intervals in subjects with apparent electrolyte imbalance were not registered.

## 2.3 Hemorheologic Examinations

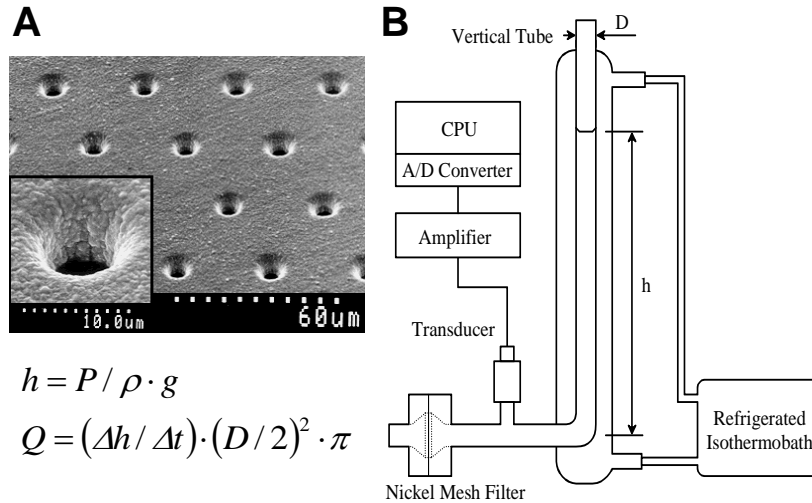
### 2.3.1 Erythrocyte suspensions

Hemorheologic investigation of erythrocyte deformability was introduced elsewhere in detail [6,10]. In brief, venous blood was sampled from antecubital vein in the morning after an overnight fast, using 21-gauge needles and disposable syringes (Terumo Japan, Tokyo, Japan) filled with 1/10 volume of 3.8% trisodium citrate as an anticoagulant on the day of ECG recording. Blood cell counting and hematocrit (Ht) measurement were performed by means of hemocytometer (Ace Counter, FLC-240A, Fukuda Denshi Co. Ltd., Tokyo, Japan). For preparing erythrocyte suspensions, supernatant was carefully aspirated to replace buffy coat and plasma with saline buffered with N-(2-hydroxyethyl)-piperazine-N'-2-ethanesulfonic acid (HEPES) sodium salt (HEPES-Na) after centrifugation at 1300 x g for 10 minutes. Composition of HEPES-Na-buffered saline (HBS) was NaCl 141 mM and HEPES-Na 10 mM. Osmolality and pH of the HBS were 287 mOsm/kg-H<sub>2</sub>O and 7.4, respectively. The osmolality of the HBS was measured using a freezing point depression type osmometer (Fiske Mark 3 Osmometer, Fiske Associates, MA, USA). Erythrocytes were then washed three times by repeated resuspension with HBS and centrifugation at 800 x g, 600 x g and 500 x g for 10 minutes, respectively. The final Ht of erythrocyte suspension was adjusted to 3.0%. These procedures were performed within 2 hours after venous blood sampling for subsequent filtration experiments.

### 2.3.2 Nickel mesh filter

Fig. 1A shows an electron microscopic photograph of a nickel mesh filter which was produced

**Figure 1. Nickel Mesh Filter and Filtration Technique**



**A:** Scanning electron microscopic photograph of a nickel mesh filter. Magnification of a single pore in nickel mesh shows the smooth transition into the pore interior (inset). **B:** Schematic illustration of gravity-based nickel mesh filtration system. Height of the meniscus within the vertical tube ( $h$ ) was obtained by continuous falling of filtration pressure ( $P$ ), specific gravity ( $\rho$ ) and acceleration of gravity ( $g$ ). Flow rate ( $Q$ ) was calculated automatically by the first time derivatives of  $h$  ( $dh/dt$ ) and internal cross sectional area of the vertical tube.  $D$ , internal diameter of vertical tube.

in accordance with our specifications by a photofabrication technique (Dainippon Printing Co. Ltd., Tokyo, Japan). We specified that this filter should have an outer diameter of 13 mm, a filtration area 8 mm in diameter, 11  $\mu\text{m}$  thick, and inter-pore distance of 35  $\mu\text{m}$  (Tsukasa Sokken Co. Ltd., Tokyo, Japan). The uniform vertical pores were distributed regularly across the filter without coincidence or branching inside the filter. The pore entrances exhibited round and smooth transition into the pore interior, which promotes smooth bending deformation of passing erythrocytes. Pore diameters are all exactly identical in a specific nickel mesh filter. Filters with a specific pore diameter ranging from 3.0 to 6.0  $\mu\text{m}$  are available and selected depending on the suspension materials. After repeated preliminary experiments to choose an appropriate pore size, a nickel mesh filter with a pore diameter of 4.94  $\mu\text{m}$  was selected in the present study.

Filtration experiments were performed blindly using a gravity-based nickel mesh filtration apparatus (Model NOBU-II, Tsukasa Sokken Co. Ltd., Tokyo, Japan) as shown in Fig. 1B. In brief, the relation between hydrostatic pressure ( $P$ ;  $\text{mmH}_2\text{O}$ ) and time ( $t$ ; sec) was obtained continuously during filtration process using a pressure transducer.  $P$  was transformed to a

height of meniscus in vertical tube (h; mm). The tangent of h-t curve gives the rate of fall of the meniscus, which is the first time derivative of the h (dh/dt). Thereafter, flow rates (Q; ml/min) was acquired by multiplying the dh/dt by the internal cross-sectional area of the vertical tube, and the complete set of flow rates (Q; ml/min) and corresponding P (P-Q relationship) was obtained<sup>7,10</sup>. This procedure was automatically performed by measurement software installed in a personal computer (DELL Latitude CS, Dell Inc., Round Rock, TX, USA) and monitored on the main window of the computer screen.

Immediately after starting data acquisition, the measurement software displays the h-t curve. When the filtration has been completed, the software displays the P-Q curve. The h-t and P-Q curves are shown on the computer screen and stored simultaneously on Microsoft Office Excel 2003 on Windows XP (Microsoft, Tokyo, Japan). Temperature of the specimens was kept at 25°C by circulating isothermal water through a water jacket surrounding the vertical tube (Fig. 1B). The percentage of the flow rate of erythrocyte suspension relative to that of HBS at a filtration pressure of 100 mmH<sub>2</sub>O was used as an index of deformability in overall erythrocytes with different age (%). These experiments were performed at room temperature (22 ± 3°C).

## 2.4 Data Analyses

All data were expressed as means ± standard deviation (SD). For statistical analyses, sample size was calculated to provide 95% power with  $\alpha$  error of 0.05 and the minimum effective dose of 0.30 based on our previous study [10], where effective dose was defined as intergroup difference of means divided by SD. Consequently, this size should have been totally ≥ 290 cases. Data sets were examined by Kolmogorov-Smirnov test and Shapiro-Wilks test for normality. Comparison of continuous variables between the two groups was conducted with unpaired Student's *t* test or Mann-Whitney U test depending on the normality. Discrete variables were analyzed as a contingency table using Fisher's exact test or Pearson's  $\chi^2$  test. Multiple comparisons among more than two groups were performed using analysis of variance (ANOVA). Stepwise multiple regression analysis was applied to determine the significant contributors to the objective variables. None of the variables with missing data qualified. The criterion for entering into the regression model was a statistical significance or otherwise clinically meaningful variables. Explanatory variables were checked for confounding factor and variance inflation factor (VIF) > 10 was defined as multicollinearity. These analyses were

**Table 1. Baseline characteristics in diabetic and control groups**

	Diabetic group (n = 215)	Control group (n = 88)	p value
Age (years)	57.6 ± 11.6	60.3 ± 7.3	0.080
Gender (females/males)	68 / 147	35 / 53	0.184
Current Smokers (yes/no)	88 / 127	26 / 62	0.069
Hypertension (yes/no)	39 / 176	21 / 67	0.269
Dyslipidemia (yes/no)	58 / 157	13 / 75	0.025
Diabetic complication			
Retinopathy (yes/no)	57 / 158	—	—
Nephropathy (yes/no)	43 / 172	—	—
Neuropathy (yes/no)	79 / 136	—	—
BMI (kg/m <sup>2</sup> )	24.6 ± 3.9	23.6 ± 3.0	0.023
Systolic BP (mmHg)	127.8 ± 12.0	132.5 ± 12.2	0.021
Diastolic BP (mmHg)	80.1 ± 11.8	82.0 ± 11.2	0.193
HbA1c(NGSP) (%)	7.76 ± 1.78	5.22 ± 0.49	< 0.001
CVRR (%)	3.10 ± 1.51	5.64 ± 1.58	< 0.001

<b>Total Cholesterol (mg/dl)</b>	209.6 ± 45.8	201.4 ± 36.1	0.101
<b>HDL Cholesterol (mg/dl)</b>	54.6 ± 15.5	57.9 ± 14.8	0.092
<b>LDL Cholesterol (mg/dl)</b>	123.5 ± 36.0	109.8 ± 29.8	0.002
<b>Triglyceride (mg/dl)</b>	169.5 ± 163.3	141.4 ± 104.4	0.137
<b>Serum K (mEq/L)</b>	4.18 ± 0.41	4.17 ± 0.44	0.917
<b>Hb (g/dl)</b>	14.1 ± 1.7	14.0 ± 1.6	0.521
<b>Ht (%)</b>	41.1 ± 4.9	40.2 ± 4.2	0.114
<b>Erythrocyte count (x 10<sup>4</sup> /μl)</b>	447.4 ± 55.5	431.1 ± 51.9	0.019
<b>Erythrocyte deformability (%)</b>	87.4 ± 3.6	88.0 ± 2.4	0.067

*BMI, body mass index calculated by body weight (kg) divided by square of height (m); BP, blood pressure; CVRR, coefficient of variance of R-R intervals in electrocardiogram reflecting autonomic nervous function; HbA1c(NGSP), hemoglobin A1c relative to the whole hemoglobin estimated according to National Glycohemoglobin Standardization Program.*

performed using Bell Curve for Excels version 2.12 (Social Survey Research Information Co., Ltd., Tokyo, Japan). Differences with two-sided  $p < 0.05$  were considered significant.

### 3. RESULTS

#### 3.1 Comparison of diabetics vs. controls

Baseline characteristics of diabetic and nondiabetic groups are detailed in Table 1. There were no significant differences between the two groups in the prevalence of hypertension and current smoking. However, dyslipidemia in the diabetic group was prevalent relative to that in control group, BMI in the former was greater than that in the latter, whereas systolic blood pressure in the former was lower than that in the latter, indicating that blood pressure was controlled well in the diabetic group. In laboratory data, HbA1c(NGSP), LDL cholesterol and RBC in the diabetic group were elevated relative to the corresponding parameters in the control group, whereas CVRR in the former was less than that in the latter. Difference of mean erythrocyte deformability in the diabetic vs. non-diabetic group did not reach the statistical significance ( $p = 0.067$ ).

Since smoking is reported to impair the erythrocyte deformability [11], this deformability in smokers were compared with that in non-smokers (Table 2). In the diabetic group, the erythrocyte deformability in the current smokers was impaired relative to that in the non-smokers ( $p = 0.045$ ), whereas this was not true in the control group. Further, the erythrocyte deformability in non-diabetic group was compared with that in diabetic subgroups that were stratified by diabetic complications (Table 3). This deformability was impaired significantly ( $p = 0.047$ ) according to the accumulation of diabetic complications (i.e., retinopathy, nephropathy and neuropathy).

#### 3.2 ECG and hemorheologic comparison

As erythrocyte deformability is influenced by many factors [6,10,12,13], this deformability was analyzed by multivariate analysis, i.e., stepwise multiple regression analysis was applied to demographic and laboratory variables including both diabetic and control groups to find covariates contributing significantly to the erythrocyte deformability under the concurrent monitoring of VIF to avoid multicollinearity. However, significant regression model was not obtained when smoking and CVRR were included into the model applied to diabetic and control subjects ( $R^2 = 0.098$ ,  $F = 1.956$  and  $p = 0.066$ ). In the limited diabetic group, multiple

**Table 2. Effects of smoking on erythrocyte deformability**

	Current smokers	Non-smokers	p value
Diabetic group (n = 215)	86.8 ± 3.9 (88)	87.8 ± 3.1 (127)	0.045
Control group (n = 88)	87.9 ± 2.6 (26)	88.1 ± 1.7 (62)	0.840

Parentheses indicate number of subjects in subgroups.

**Table 3. Comparison of erythrocyte deformability in controls and diabetic patients**

	n	Erythrocyte deformability	p value
Control patients	88	88.0 ± 2.4	0.047
Diabetic patients without complications	73	87.6 ± 2.9	
with one complication	70	87.7 ± 3.2	
with two complications	44	86.9 ± 4.2	
with all complications	28	86.4 ± 10.4	

Diabetic complications mean triopathy including retinopathy, nephropathy and neuropathy.

**Table 4. Multiple regression analysis predicting contributors to the erythrocyte deformability**

Covariates	$\beta$	standardized $\beta$	95%CI	F value	p value
HbA1c	-0.287	-0.162	-0.531 — -0.042	5.346	0.022
triglyceride	-0.003	-0.159	-0.006 — 0.000	5.209	0.024
QTc interval	-13.084	-0.093	-32.377 — 6.208	1.789	0.183

This multiple regression model was applied to diabetic patients (n = 215) showing  $R^2 = 0.075$ ,  $F = 5.300$  and  $p = 0.002$ .

**Table 5. Multiple regression analysis predicting contributors to the QTc interval**

Covariates	$\beta$	standardized $\beta$	95%CI	F value	p value
CVRR	-0.004	-0.293	- 0.006 — - 0.002	18.1	< 0.001
BMI	0.001	0.141	0.000 — 0.002	4.1	0.044
HbA1c	0.002	0.136	0.000 — 0.004	3.7	0.055
Erythrocyte deformability	-0.001	-0.112	- 0.002 — 0.000	2.6	0.109

This multiple regression model was applied to diabetic patients (n = 215) showing  $R^2 = 0.130$ ,  $F = 6.884$  and  $p < 0.001$ .

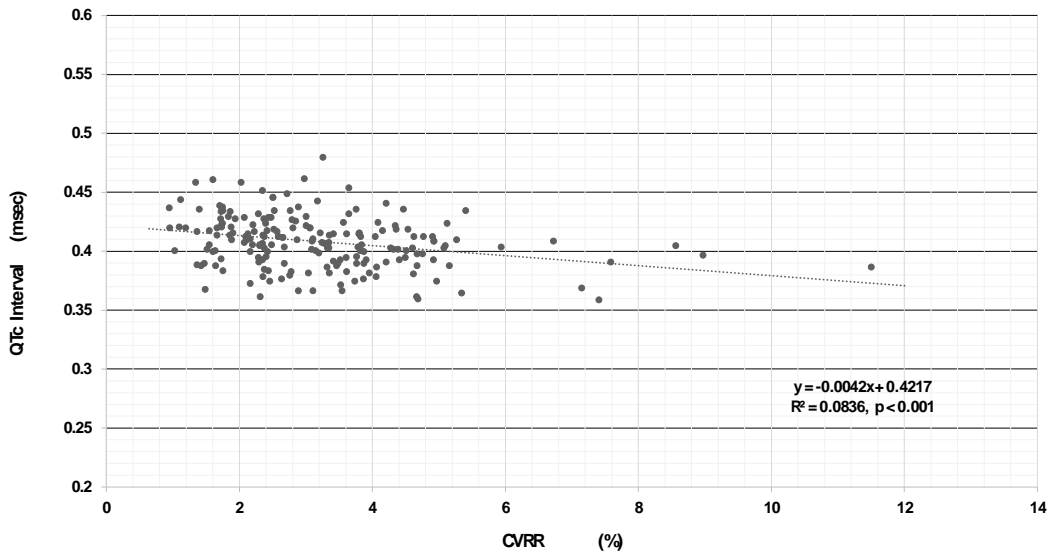
regression analysis demonstrated that HbA1c ( $p = 0.022$ ) and triglyceride ( $p = 0.024$ ) were the best contributors to the erythrocyte deformability impairment (Table 4), whereas QTc interval prolongation as a measure of diabetic microvascular dysfunction had no significant contribution to the diabetic erythrocyte deformability ( $p = 0.183$ ). Likewise, QTc intervals of ECG recorded in diabetic patients and control subjects were fitted to the multiple regression model. However, clinically relevant model was obtained only when this analysis was applied to the diabetic group alone, i.e., best regression model demonstrated that CVRR ( $p < 0.001$ ) and BMI ( $p = 0.044$ ) were the significant contributors to the QTc intervals (Table 5). Again, diabetic erythrocyte deformability was not a direct contributor to the QTc intervals ( $p = 0.109$ ). Although QTc intervals is influenced by serum electrolytes imbalance, the regression model including serum K concentration did not reach statistical significance ( $R^2 = 0.099$ ,  $F = 1.800$  and  $p = 0.121$ ).

## 4. DISCUSSION

The present study investigated electrocardiographic and hemorheologic correlation in patients with type 2 diabetes. Main findings of this study are 1) clustering of diabetic complications and current smoking caused poor erythrocyte deformability, 2) HbA1c (NGSP) was mostly attributable to the poor diabetic erythrocyte deformability, and 3) the QTc intervals prolongation was associated with reduced CVRR in diabetic patients. However, direct correlation between the erythrocyte deformability and diabetic microvascular dysfunction was not obtained.

It is generally accepted that erythrocyte deformability is mainly determined by 1) the erythrocyte membrane properties, 2) the erythrocyte internal viscosity and 3) the cellular geometric factors reflected by erythrocyte shape and volume (surface-to-volume ratio).

**Figure 2. Relationship between CVRR and QTc Interval**

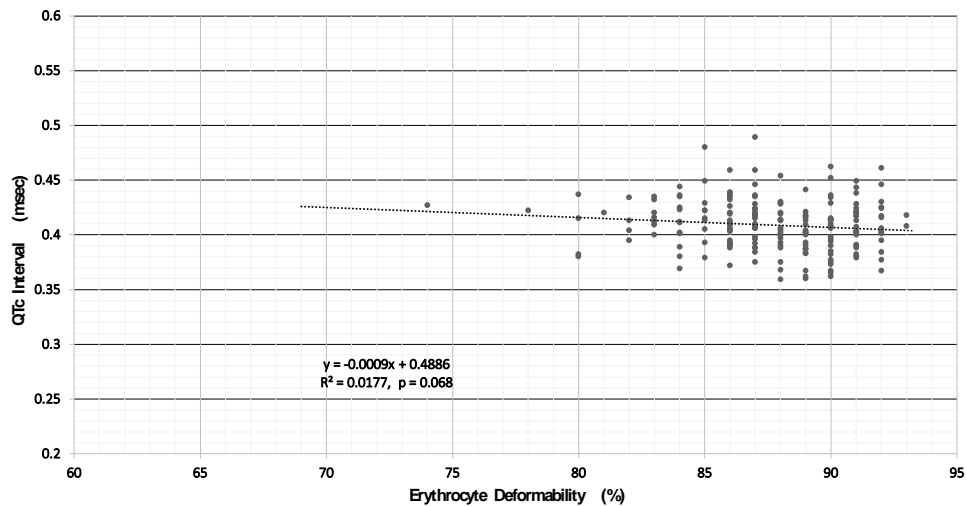


*Cross-sectional correlation between the CVRR (%) and the QTc intervals (msec) recorded by digital electrocardiogram (ECG). Regression equation and correlation coefficient are indicated ( $r = -0.277, p < 0.001$ ).*

Therefore, the erythrocyte deformability is impaired by elevated membrane rigidity, increased internal viscosity or several kinds of shape changes alone or in concert [14,15]. In literature, morphological changes in diabetic erythrocytes have been reported in atomic force microscopic investigation, which include decreased biconcave depth, diameter and height [3]. Diabetic erythrocyte membrane shows phospholipid peroxidation and decreased membrane ion-transporting enzymatic activities [16]. Further, non-enzymatic glycation of hemoglobin (Hb) alters the fine conformation and secondary structure of native Hb [17], which may influence the hemorheological behaviors of circulating erythrocytes. These findings underlie the poor deformability, low flow velocity and short lifespan in circulating diabetic erythrocytes [4,10,18].

Erythrocyte deformability is a major determinant of microcirculation, and hence poor deformability causes tissue hypoxia. The difference in the deformability between the controls and diabetes did not reach the significance ( $p = 0.067$ ) by our sensitive and quantitative nickel mesh filter (Fig. 1A). This is attributable partly to the intensive antidiabetic treatment in the heterogeneous diabetic patients. Actually, impairment of erythrocyte deformability in diabetic patients with smoking and clustering complications was evident (Tables 1 and 2). One of main factors linking smoking and progression of diabetic complication is oxidative damage [11], i.e., human erythrocytes carrying oxygen are susceptible to the oxidative stress [19-21], which is deeply involved in the pathogenesis of type 2 diabetes [22,23]. HbA1c and triglyceride were the major determinants of diabetic erythrocyte deformability (Table 4). Although the reason is not clear, the deformability was most sensitive to the serum triglyceride level in apparently healthy volunteers with various lipid profiles [6]. Erythrocyte deformability is impaired in diabetic patients in literature [10,24]. This impairment is ameliorated by antidiabetic treatment [25], whereas it is aggravated by clustering of diabetic complications [26], which indicate close link between abnormal erythrocyte behavior and diabetic microangiopathy.

**Figure 3. Relationship between Erythrocyte Deformability and QTc Interval**



Cross-sectional correlation between the erythrocyte deformability (%) and the QTc intervals (msec) recorded by digital ECG. Regression equation and correlation coefficient are indicated ( $r = -0.137, p = 0.068$ ).

Type 2 diabetes is associated with microvascular complications, which are reflected partly by QTc interval prolongation [27]. QTc interval is lengthened according to the progression of autonomic nervous dysfunction as demonstrated in this study (Figure 2). Actually, this interval is a simple and reliable ECG parameter to predict future cardiac event and mortality in the elderly with frailty [28] and in the patients with sickle cell disease, which is a representative hereditary disease showing marked erythrocyte deformability impairment and systemic microvascular occlusion [29]. Reportedly, vascular endothelial function is related to the QTc intervals, and the QTc interval prolongation is associated with coronary microvascular dysfunction in patients with chest pain and normal coronary trees (so-called cardiac syndrome X) [30]. In our study, QTc intervals are explained mostly by the combination of CVRR, BMI and HbA1c (Table 5), which is compatible to that QTc intervals

are an overall surrogate of diabetic microvascular and autonomic abnormality [31]. Studies investigating hemorheologic and ECG correlations are rare, and the present study explored the relationship between QTc intervals and erythrocyte deformability (Figure 3). Direct negative correlation between the two parameters did not reach statistical significance ( $r = -0.137$ ,  $p = 0.068$ ), indicating further investigations are required to verify the hypothesis that erythrocytes rheology is important to maintain the physiological microvascular function.

This cross-sectional study contains a few limitations, i.e., the control group includes non-diabetic patients who are not necessarily healthy leading to the marginal significance in the intergroup difference of erythrocyte deformability between the diabetic and non-diabetic patients (Table 1). Antidiabetic medication and education are under the discretion of the treating physician. An extent of smoking and the severity of diabetic triopathy are not semi-quantified. Percentage of current smokers are high relative to the standard of this country, i.e., the treating physicians should have encouraged their outpatients in smoking secession program. Finally, we adopted QTc interval as a naive surrogate marker of microvascular dysfunction in diabetic patients as in literature [27,31]. More sophisticated parameters such as index of microcirculatory resistance may have yielded clear correlation between the erythrocyte deformability and microvascular dysfunction [32].

## **5. CONCLUSION**

The present study using the nickel mesh filtration technique investigated ECG and hemorheologic correlation in patients with type 2 diabetes under medication. Erythrocyte deformability was impaired in diabetic smokers and in diabetic patients with complications. This abnormal erythrocyte behavior presumably underlies disturbed microcirculation and progression of diabetic microangiopathy. Impaired diabetic erythrocyte deformability was dependent on HbA1c, but direct correlation between the impaired deformability and microvascular dysfunction was not obtained in the diabetic patients group. Further studies are required to assess the exact interaction between the abnormal erythrocytes rheology and diabetic microvascular dysfunction using current sophisticated parameters.

### **COMPETING INTERESTS DISCLAIMER:**

Authors have declared that no competing interests exist. The products used for this research are commonly and predominantly use products in our area of research and country. There is absolutely no conflict of interest between the authors and producers of the products because we do not intend to use these products as an avenue for any litigation but for the advancement of knowledge. Also, the research was not funded by the producing company rather it was funded by personal efforts of the authors.

## **REFERENCES**

1. Cuschieri S. Type 2 diabetes – an unresolved disease across centuries contributing to a public health emergency. *Diabetes Metab Syndr*. 2019; 13: 450-3.
2. Caimi G, Presti RL. Techniques to evaluate erythrocyte deformability in diabetes mellitus. *Acta Diabetol*. 2004; 41: 99-103.
3. Loyola-Leyva A, Loyola-Rodríguez JP, Atzori M, González FJ. Morphological changes in erythrocytes of people with type 2 diabetes mellitus evaluated with atomic force microscopy: a brief review. *Micron*. 2018; 105: 11-7.

4. Tsukada K, Sekizuka E, Oshio C, Minamitani H. Direct measurement of erythrocyte deformability in diabetes mellitus with a transient microchannel capillary model and high-speed video camera system. *Microvasc Res.* 2001; 61: 231-9.
5. Moon JS, Kim JH, Kim JH, Park IR, Lee JH, Kim HJ, et al. Impaired RBC deformability is associated with diabetic retinopathy in patients with type 2 diabetes. *Diabetes Metab.* 2016; 42: 448-52.
6. Ejima J, Ijichi T, Ohnishi Y, Maruyama T, Kaji Y, Kanaya S, et al. Relationship of high-density lipoprotein cholesterol and red blood cell filterability: cross-sectional study of healthy subjects. *Clin Hemorheol Microcirc.* 2000; 22: 1-7.
7. Ariyoshi K, Maruyama T, Odashiro K, Akashi K, Fujino T, Uyesaka N. Impaired erythrocyte filterability of spontaneously hypertensive rats: investigation by nickel mesh filtration technique. *Circ J.* 2010; 74: 129-36.
8. Yokoyama A. Prognostic significance of QT prolongation and autonomic nervous dysfunction in alcoholics with diabetes mellitus. *Keio J Med.* 1993; 42: 141-8.
9. Ohta Y, Tsuchihashi T, Onaka U, Hasegawa E. Clustering of cardiovascular risk factors and blood pressure control status in hypertensive patients. *Intern Med.* 2010; 49: 1483-7.
10. Saito K, Kokawa Y, Fukata M, Odashiro K, Maruyama T, Akashi K, et al. Impaired deformability of erythrocytes in diabetic rat and human: investigation by the nickel-mesh-filtration technique. *J Biorheol.* 2011; 25: 18-26.
11. Hausteil KO, Krause J, Hausteil H, Rasmussen T, Cort N. Effects of cigarette smoking or nicotine replacement on cardiovascular risk factors and parameters of haemorheology. *J Intern Med.* 2002; 252: 130-9.
12. Odashiro K, Maruyama T, Yokoyama T, Nakamura H, Fukata M, Yasuda S, et al. Impaired erythrocyte deformability in patients with coronary risk factors: significance of nonvalvular atrial fibrillation. *J Atr Fibrillation.* 2013; 6: 939 doi: 10.4022/jafib.939.
13. Odashiro K, Saito K, Arita T, Maruyama T, Fujino T, Akashi K. Impaired deformability of circulating erythrocytes obtained from nondiabetic hypertensive patients: investigation by a nickel mesh filtration technique. *Clin Hypertens.* 2015; 21: 17. doi: 10.1186/s40885-015-0030-9.
14. Mohandas N, Chasis JA. Red cell deformability, membrane material properties and shape: regulation by transmembrane, skeletal and cytosolic proteins and lipids. *Semin Hematol.* 1993; 30: 171-92.
15. Hiruma H, Noguchi CT, Uyesaka N, Schechter AN, Rodgers GP. Contributions of sickle hemoglobin polymer and sickle cell membranes to impaired filterability. *Am J Physiol.* 1995; 268: H2003-8.
16. Rajeswari P, Natarajan R, Nadler JL, Kumar D, Kalra VK. Glucose induces lipid peroxidation and inactivation of membrane-associated ion-transport enzymes in human erythrocytes in vivo and in vitro. *J Cell Physiol.* 1991; 149: 100-9.
17. Ye S, Ruan P, Yong J, Shen H, Liao Z, Dong X. The impact of the HbA1c level of type 2 diabetics on the structure of hemoglobin. *Sci Rep.* 2016; 6: 33352. doi: 10.1038/srep33352.

18. Huang Z, Liu Y, Mao Y, Chen W, Xiao Z, Yu Y. Relationship between glycated haemoglobin concentration and erythrocyte survival in type 2 diabetes mellitus determined by a carbon monoxide breath test. *J Breath Res.* 2018; 12: 026004. doi: 10.1088/1752-7163/aa9081.
19. Uyesaka N, Hasegawa S, Ishioka N, Ishioka R, Shio H, Schechter AN. Effects of superoxide anions on red cell deformability and membrane proteins. *Biorheology.* 1992; 29: 217-29.
20. Iwata H, Ukeda H, Maruyama T, Fujino T, Sawamura M. Effect of carbonyl compounds on red blood cells deformability. *Biochem Biophys Res Comm.* 2004; 321: 700-6.
21. Okamoto K, Maruyama T, Kaji Y, Harada M, Mawatari S, Fujino T, et al. Verapamil prevents impairment in filterability of human erythrocytes exposed to oxidative stress. *Jpn J Physiol.* 2004; 54: 39-46.
22. Robson R, Kundur AR, Singh I. Oxidative stress biomarkers in type 2 diabetes mellitus for assessment of cardiovascular disease risk. *Diabetes Metab Syndr.* 2018; 12: 455-62.
23. Thakur P, Kumar A, Kumar A. Targeting oxidative stress through antioxidants in diabetes mellitus. *J Drug Target.* 2018; 26: 766-76.
24. Linderkamp O, Ruef P, Zilow EP, Hoffmann GF. Impaired deformability of erythrocytes and neutrophils in children with newly diagnosed insulin-dependent diabetes mellitus. *Diabetologia.* 1999; 42: 865-9.
25. Forst T, Weber MM, Löbig M, Lehmann U, Müller J, Hohberg C, et al. Pioglitazone in addition to metformin improves erythrocyte deformability in patients with type 2 diabetes mellitus. *Clin Sci (Lond).* 2010; 119: 345-51.
26. Shin S, Ku YH, Ho JX, Kim YK, Suh JS, Singh M. Progressive impairment of erythrocyte deformability as indicator of microangiopathy in type 2 diabetes mellitus. *Clin Hemorheol Microcirc.* 2007; 36: 253-61.
27. Kobayashi S, Nagao M, Asai A, Fukuda I, Oikawa S, Sugihara H. Severity and multiplicity of microvascular complications are associated with QT interval prolongation in patients with type 2 diabetes. *J Diabetes Investig.* 2018; 9: 946-51.
28. Ma T, Cai J, Zhu YS, Chu XF, Wang Y, Shi GP, et al. Association between a frailty index based on common laboratory tests and QTc prolongation in older adults. *Clin Interv Aging.* 2018; 13: 797-804.
29. Indik JH, Nair V, Rafikov R, Nyotowidjojo IS, Bisla J, Kansal M, et al. Associations of prolonged QTc in sickle cell disease. *PLoS One.* 2016; 11: e0164526
30. Sara JD, Lennon RJ, Ackerman MJ, Friedman PA, Noseworthy PA, Lerman A. Coronary microvascular dysfunction is associated with baseline QTc prolongation amongst patients with chest pain and non-obstructive coronary artery disease. *J Electrocardiol.* 2016; 49: 87-93.
31. Ninkovic VM, Ninkovic SM, Miloradovic V, Stanojevic D, Babic M, Giga V, et al. Prevalence and risk factors for prolonged QT interval and QT dispersion in patients with type 2 diabetes. *Acta Diabetol.* 2016; 53: 737-44.

32. Chung JH, Lee KE, Park JW, Shin ES: Coronary microvascular disease and clinical prognosis in deferred lesions: the index of microcirculatory resistance. Clin Hemorheol Microcirc. 2019; 71: 137-40.

UNDER PEER REVIEW